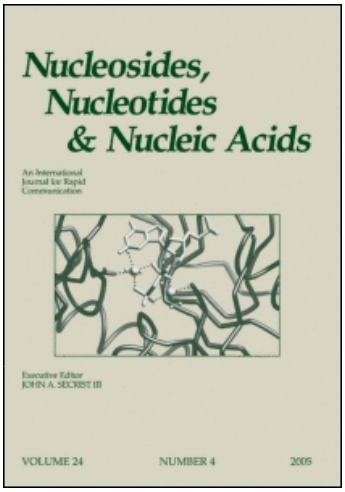


**Nucleosides, Nucleotides and Nucleic Acids**
Publication details, including instructions for authors and subscription information:
http://www.informaworld.com/smpp/title~content=t713597286

# Structure and Stability of an Oligonucleotide Containing 2'-Deoxy-6-thioguanosine

Michael S. Christopherson[a]; Arthur D. Broom[a]
[a] Department of Medicinal Chemistry, University of Utah Salt, Lake City, Utah

**To cite this Article** Christopherson, Michael S. and Broom, Arthur D.(1994) 'Structure and Stability of an Oligonucleotide Containing 2'-Deoxy-6-thioguanosine', Nucleosides, Nucleotides and Nucleic Acids, 13: 1, 351 — 368
**To link to this Article: DOI:** 10.1080/15257779408013246
**URL:** http://dx.doi.org/10.1080/15257779408013246

NUCLEOSIDES & NUCLEOTIDES, 13(1-3), 351-368 (1994)

# STRUCTURE AND STABILITY OF AN OLIGONUCLEOTIDE CONTAINING 2'-DEOXY-6-THIOGUANOSINE

**Michael S. Christopherson and Arthur D. Broom***
**Department of Medicinal Chemistry, University of Utah**
**Salt Lake City, Utah 84112**



## ABSTRACT

Structure and stability of the self-complementary octamers d(AAACGTTT) and d(AAAC$s^6$GTTT) have been evaluated by one and two-dimensional NMR and UV techniques. Temperature dependence studies by NMR and UV indicate the presence of 2'-deoxy-6-thioguanosine ($ds^6G$) acts to destabilize duplex formation in the octamer by about 10 to 15°C. Comparison of octamers indicate the presence of $ds^6G$ octamer acts to induce structural perturbations that are not localized to the central dC-$ds^6G$ base pairs but affect the overall structure of the entire octamer.

## INTRODUCTION

The purine antimetabolite 6-thioguanine has been used for more than 30 years for treatment of human malignancies, especially leukemias.[1] Despite widespread use of thioguanine, the precise molecular basis of its action is not entirely clear. Evidence from several research groups has established incorporation of thioguanine into DNA as a major requirement for anticancer activity of this purine antimetabolite.[2-7] These correlations between incorporation into DNA and cytotoxicity have found some physicochemical basis from studies describing the overall effect of incorporation into nucleic acids in place of guanine. Replacement of guanine with 6-thioguanine in polyribonucleotides results in dramatic helix destabilization.[8] It has been proposed that the increased van der Waals radius of sulfur and the increased length of the $C^6$-S bond length in 6-thioguanine versus the $C^6$-O

---

**Dedicated to the memory of Roland K. Robins, Ph.D**

bond of guanine result in significant distortion of hydrogen bonds which could lead to alterations of helical structure.[9] Our goal has been to define more clearly the structural changes induced by 6-thioguanine incorporation into DNA and to understand how these structural changes can account for its anticancer activity.

To examine structural changes that accompany incorporation of 6-thioguanine in place of guanine, we have developed synthetic methodology that permits site-specific incorporation of ds$^6$G into DNA.[10] A similar approach was subsequently reported by Waters and Connolly;[11] an alternative procedure was described by Xu et al.[12] Our methodology was developed to prevent the oxidative loss of sulfur known to occur in 6-thioguanine-containing oligonucleotides. Through the application of this methodology in conjunction with automated DNA synthesis technology, it is possible to synthesize sufficient quantities of DNA to enable structural characterization by high-field NMR spectroscopy. We have synthesized 10 μmol quantities of d(AAACs$^6$GTTT) (ds$^6$G octamer) as well as d(AAACGTTT) (dG octamer). By comparing NOESY spectra generated from the two self-complementary oligonucleotides, it is possible to examine structural changes induced by incorporation of 6-thioguanine in place of guanine. By examining changes in chemical shift, NOE intensities and coupling constants derived from the double-quantum filtered COSY experiment (DQF-COSY), it is possible to examine ds$^6$G-induced structural changes on a molecular level.

We have also examined changes in duplex stability accompanying 6-thioguanine incorporation. This was accomplished by using temperature-dependent UV and NMR spectroscopic methods. Potential oxidative loss of sulfur from ds$^6$G during thermal melting studies was also examined in an attempt to derive conditions that would preserve the thione of ds$^6$G at elevated temperatures in solution. This study was designed to elucidate structural consequences of dG versus ds$^6$G incorporation with the hope of providing evidence for a molecular mechanism of action of 6-thioguanine.

## MATERIALS AND METHODS

### Oligonucleotide Synthesis and Purification

The self-complementary oligonucleotide d($A_1A_2A_3C_4G_5T_6T_7T_8$) was synthesized by phosphoramidite chemistry on a 10 μmol scale using an ABI DNA synthesizer and deprotected with concentrated ammonium hydroxide under standard automated DNA synthesis conditions. After deprotection, the oligonucleotide was purified by reverse-phase HPLC using a Keystone ODS-H semi-preparative column and an isocratic mobile phase of 81% 50

mM aq. ammonium bicarbonate and 19% acetonitrile at a flow rate of 1 mL/min. The purified material was lyophilized several times from water and was subjected to structural characterization by UV and NMR spectroscopy. The $ds^6G$ containing the oligonucleotide $d(A_1A_2A_3C_4s^6G_5T_6T_7T_8)$ was synthesized on a 10 μM scale with the ABI DNA synthesizer using the $S^6$-cyanoethyl-5'-O-dimethoxytrityl-N $^2$-phenoxyacetyl-2'-deoxy-6-thioguanosine diisopropylaminocyanoethyl phosphoramidite and characterized as previously described.[10]

**UV Spectroscopy**

Thermal melting studies were conducted on a Beckman DU-8 spectrophotometer or a Hewlett Packard Diode-Array spectrophotometer, each equipped with a Peltier temperature control device. $T_m$ curves were obtained by dissolving approximately 1 O.D. of DNA in either 20 mM NaPhos (pH 7) with 0.1 M NaCl or 20 mM NaPhos (pH 7) with 1.0 m NaCl. The solutions were heated to 60°C and cooled slowly to room temperature. The temperature was ramped from 6° to 60°C at a rate of 0.5°C/min while absorbance at 260 nm was monitored. $T_m$ was determined by plotting the first derivative of each absorbance versus temperature plot utilizing the software provided with each spectrophotometer. The HPLC analysis of $d(AAACs^6GTTT)$ degradation during the $T_m$ analysis was conducted on a Supelco LC018S (5 μ) column in a gradient of 0.1 M triethylammonium bicarbonate (pH 7) in $CH_3CN$ (1-30% over 20 min) at 1 mL/min.

**NMR Spectroscopy**

One and two-dimensional proton data sets were collected on a Varian Unity 500 spectrometer. Proton chemical shifts were referenced relative to 2,2-dimethyl-2-silapentane-sulfonic acid (DSS). The oligonucleotides (2 mM in duplex) were annealed by heating to 60°C and slowly cooling to room temperature in the NMR tube. Temperature-dependent one-dimensional experiments were conducted on oligonucleotides in NaPhos buffer (pH 6). One-dimensional temperature-dependent 500 MHz $^1H$ data sets were collected in 90% $H_2O$ buffer/10% $D_2O$ employing water suppression by solvent presaturation. One-dimensional proton-decoupled 81 MHz $^{31}P$ data sets were collected in buffered 100% $D_2O$ at 10°C using an IBM AF200 spectrometer. The material was lyophilized twice from 99.9% $D_2O$ and then dissolved in 400 μL of 99.996% $D_2O$ containing 100 mM NaCl and 20 mM phosphate buffer, pH 6. Two-dimensional phase-sensitive NOESY spectra of the 8-mer were collected at 10°C (to assure duplex formation) using 50 or 150 ms mixing times, a spectral width of 5000 Hz, and a 90° pulse width of 11 ms.[13] The data sets were acquired in hypercomplex mode with 800 $t_1$ increments, 32 scans/fid, and 2048 complex points in $t_2$. The $t_2$ dimen-

sion was processed with a gaussian filter and 1 Hz of line broadening. The $t_1$ increments were zero filled to 2048 points and transformed with a gaussian apodization function. Two-dimensional proton phase-sensitive DQF-COSY spectra in $D_2O$ were collected at 10°C using the standard pulse sequence with a 1.95 second pulse repetition time, a sweep width of 5097 Hz, a 90° pulse of 10 ms, and a homospoil time of 1 ms. The data sets were acquired in a hypercomplex mode with 400 $t_1$ increments, 96 scans/fid, and 2048 complex points in $t_2$. The $t_2$ dimension was processed with a gaussian filter. The $t_1$ increments were zero filled to 2048 points and transformed with a gaussian apodization function.

## RESULTS AND DISCUSSION

### NMR Spectroscopy

By examining the effect of decreasing temperature on the appearance and line width of hydrogen-bonded imino protons, it is possible to derive information on duplex stability. The line width of the imino protons reflects the rate of proton exchange with water and is thus related to stability of the base pair.[14] The octamers were dissolved in 90% $H_2O$/10% $D_2O$ containing 0.1 M NaCl, 20 mM potassium phosphate (pH 6) and $^1H$ spectra were collected using a water suppression pulse sequence. The samples were annealed in the probe as the spectra were monitored for the appearance of imino signals. The effect of the decreasing temperature on the imino signals of the dG and $ds_6G$ octamers may be seen in Figures 1 and 2. The dG octamer (Figure 1) begins to exhibit hydrogen-bonded imino protons at 35°C while the $ds^6G$ octamer (Figure 2) does not begin to exhibit imino signals until the temperature reaches 15°C. It is also interesting to note the differences in chemical shift of the dG-dC and $ds^6G$-dC base paired protons. The $ds^6G$-dC base pair imino proton (at 11.1 ppm) appears over a full 1 ppm upfield from the dG-dC base pair imino proton (at 12.4 ppm). These data provide further evidence for the weak $ds^6G$-dC base pair, since strongly hydrogen bonded N-H protons resonate downfield from similar nonhydrogen bonded protons.[15,16] It is also interesting that the imino proton arising from the second dA-T base pair ($dA_2$-$T_7$) at about 13.8 ppm is visible in the dG octamer but not in the $ds^6G$ octamer, as can be seen by comparing Figures 1 and 2.

A plot of the line width at half-height of the imino proton signals versus temperature is shown in Figure 3. The signal line width of an imino proton involved in hydrogen binding will decrease until the exchange reaches a constant rate and a stable hydrogen bond is formed. The exchange of the dG-dC base pair in the dG octamer reaches a constant rate

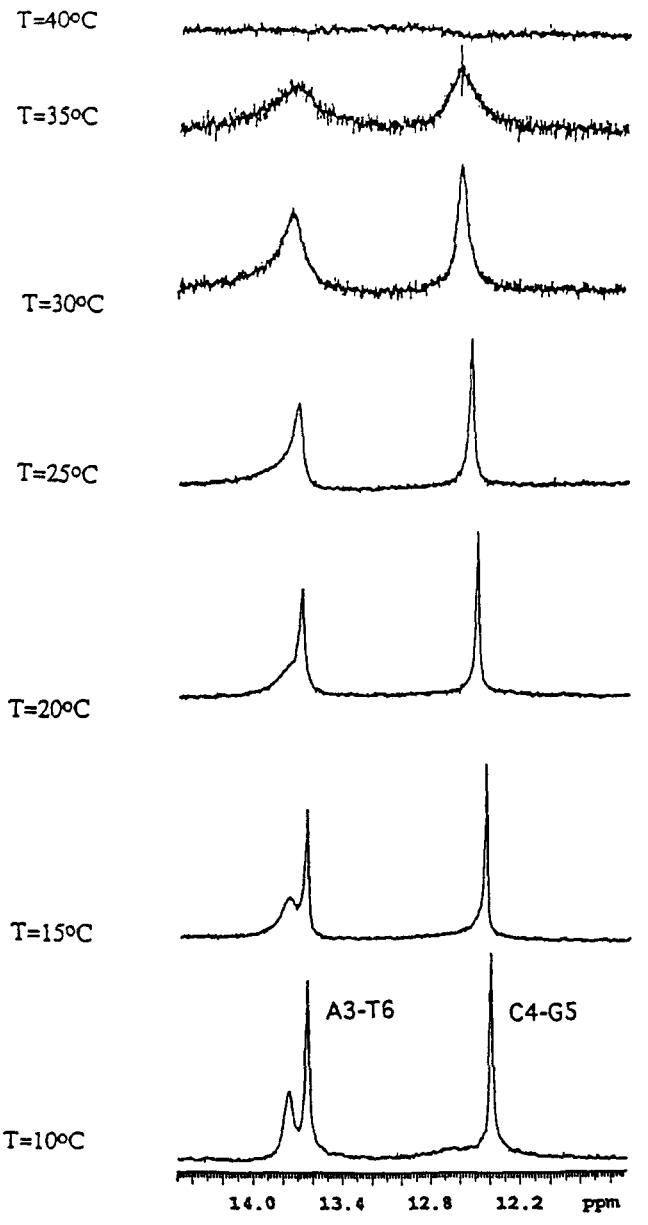


Figure 1. Temperature dependence of the 100 mHz low-field spectra (imino resonances) of d(AAACGTTT) in 0.1 M NaCl 20 mM buffer (pH 6)

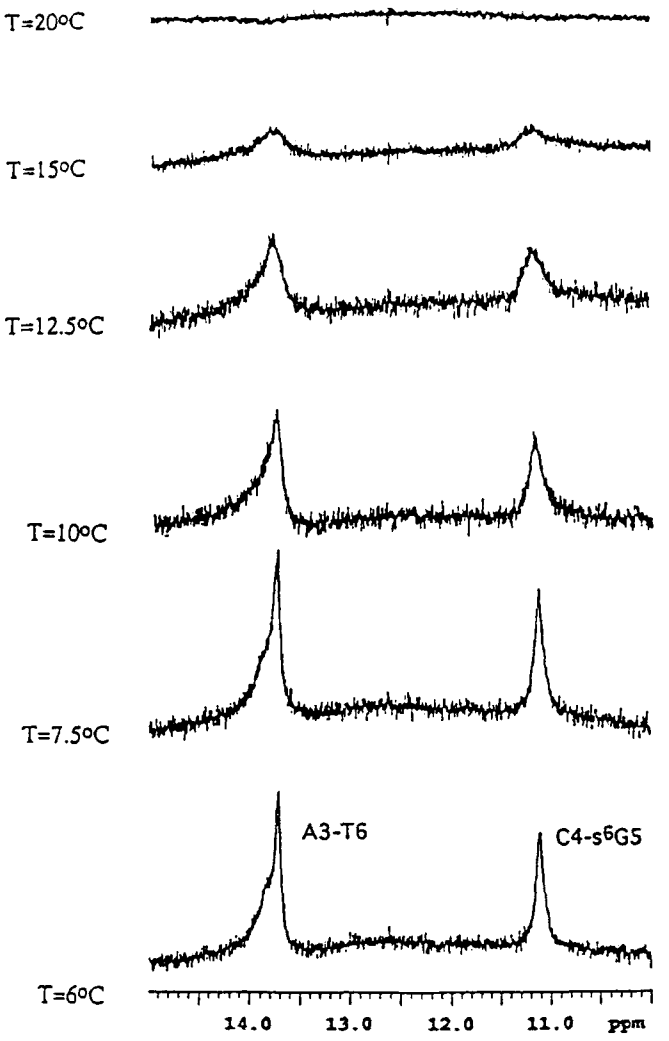


Figure 2. Temperature dependence of the 500 MHz low-field spectra (imino resonances) of d(AAACs$^6$GTTT) in 0.1 M NaCl 20 mM buffer (pH 6)

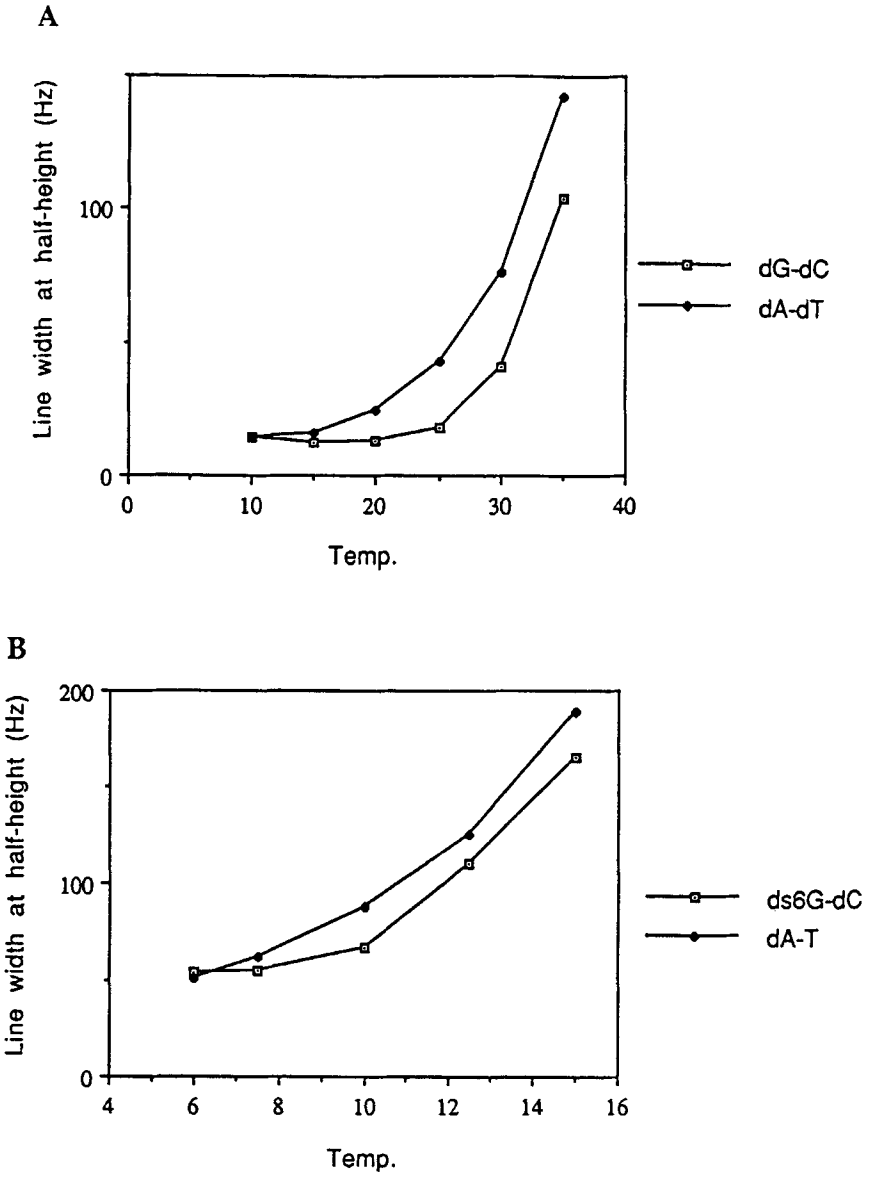


**Figure 3.** (A) Line width at half-height vs. temperature for the dG-dC and dA-T base pairs in d(AAACGTTT), (B) and the ds$^{6}$G-dC and dA-T base pairs in d(AAACs$^{6}$GTTT).

**Table 1.** Nonexchangeable $^1H$ chemical shifts (ppm) of d(AAACs$^6$GTTT) in $D_2O$ containing 0.1 M NaCl, 20 mM potassium phosphate buffer (pH 6.0) at 10°C

| | H8 | H6 | H5/CH3 | H1' | H2', H2" | H3' | H4' |
|---|---|---|---|---|---|---|---|
| A1 | 7.70 | | | 5.53 | 2.12, 2.35 | 4.53 | 3.90 |
| A2 | 7.84 | | | 5.43 | 2.38, 2.47 | 4.72 | 4.08 |
| A3 | 7.78 | | | 5.83 | 2.26, 2.52 | 4.69 | 4.16 |
| C4 | | 6.86 | 4.87 | 5.20 | 1.70, 2.01 | 4.44 | 3.87 |
| s$^6$G5 | 7.56 | | | 5.63 | 2.28, 2.44 | 4.61 | 4.06 |
| T6 | | 7.01 | 0.90 | 5.82 | 1.87, 2.27 | 4.57 | 3.95 |
| T7 | | 7.24 | 1.35 | 5.91 | 1.94, 2.28 | 4.58 | 3.91 |
| T8 | | 7.15 | 1.30 | 5.98 | 2.00, 2.00 | 4.30 | 3.74 |



at 25°C while the ds$^6$G-dC base pair in the ds$^6$G octamer does not reach a plateau until 10°C. This indicates the dG octamer has a melting temperature about 15°C higher than the ds$^6$G octamer. The presence of the ds$^6$G-dC base pair in the ds$^6$G octamer also has a destabilizing effect on the dA-T base pair. The line width of the dA-T base paired imino proton resonance continues to decrease even at 8°C. It is clear from these data that the ds$^6$G-dC base pair has a strongly destabilizing effect on the overall stability of the octamer.

High-field two-dimensional NMR techniques were used to characterize further the structural changes induced by 6-thioguanine incorporation into DNA. We carried out 10 μmol syntheses of d(AAACs$^6$GTTT) and d(AAACGTTT) through the use of automated DNA synthesis. Each octamer was purified by HPLC, lyophilized from water several times to ensure removal of buffer salts, dissolved in deuterium oxide containing 0.1 M NaCl, 20 mM potassium phosphate buffer (pH 6) and subjected to NMR spectroscopy. Two-dimensional phase-sensitive NOESY spectra of the octamers were collected at 10°C initially using a 150 ms mixing time and a spectral width of 5000 Hz. All of the expected aromatic-

Table 2. Nonexchangeable $^1H$ chemical shifts (ppm) of d(AAACGTTT) in $D_2O$ containing 0.1 M NaCl, 20 mM potassium phosphate buffer (pH 6.0) at 10°C

| | H8 | H6 | H5/CH3 | H1' | H2', H2" | H3' | H4' |
|---|---|---|---|---|---|---|---|
| A1 | 7.73 (0.03)* | | | 5.52 (0.01) | 2.15, 2.38 (0.03, 0.03) | 4.54 (0.01) | 3.90 (0) |
| A2 | 7.86 (0.02) | | | 5.48 (0.05) | 2.41, 2.53 (0.03, 0.06) | 4.73 (0.01) | 4.09 (0.02) |
| A3 | 7.80 (0.02) | | | 5.81 (0.02) | 2.27, 2.52 (0.01, 0) | 4.70 (0.01) | 4.15 (0.01) |
| C4 | | 6.85 (0.01) | 4.80 (0.07) | 5.23 (0.03) | 1.63, 2.01 (0.07, 0.01) | 4.47 (0.03) | 3.84 (0.03) |
| G5 | 7.52 (0.04) | | | 5.66 (0.03) | 2.31, 2.46 (0.03, 0.02) | 4.64 (0.03) | 4.06 (0) |
| T6 | | 6.98 (0.03) | 1.06 (0.16) | 5.75 (0.07) | 1.81, 2.26 (0.06, 0.01) | 4.55 (0.02) | 3.93 (0.02) |
| T7 | | 7.20 (0.04) | 1.34 (0.01) | 5.88 (0.03) | 1.91, 2.27 (0.03, 0.01) | 4.57 (0.01) | 3.87 (0.04) |
| T8 | | 7.11 (0.04) | 1.27 (0.03) | 5.96 (0.02) | 1.97, 2.01 (0.03, 0.01) | 4.29 (0.01) | 3.71 (0.03) |

* Value in parentheses represents the absolute value difference in chemical shift between the dG and ds$^6$G octamers.



H1' cross-peaks were clearly resolved in both spectra which made assignments possible based on sequence-specific assignment techniques.[10,13] A summary of the assignments for both ds$^6$G and dG-containing octamers is presented in Tables 1 and 2.

One way to characterize the structural differences existing between the octamers is to examine the differences in the chemical shift of the assigned resonances. In parentheses, Table 2 contains the absolute value of the chemical shift differences between the ds$^6$G and dG octamers. While small chemical shift differences exist in all eight of the bases, it is clear the largest differences exist in $C_4$ and $T_6$, the bases 5' and 3' to ds$^6$G. If the incorporation of ds$^6$G into DNA were to induce structural changes, we would expect to see the most profound effects on the bases nearest its position. Results in Table 2 support this hypothesis.

Another way to examine differences in structure of the dG/ds$^6$G octamers is to examine the size of the NOE cross-peaks generated in the NOESY spectra. Figures 4 and 5

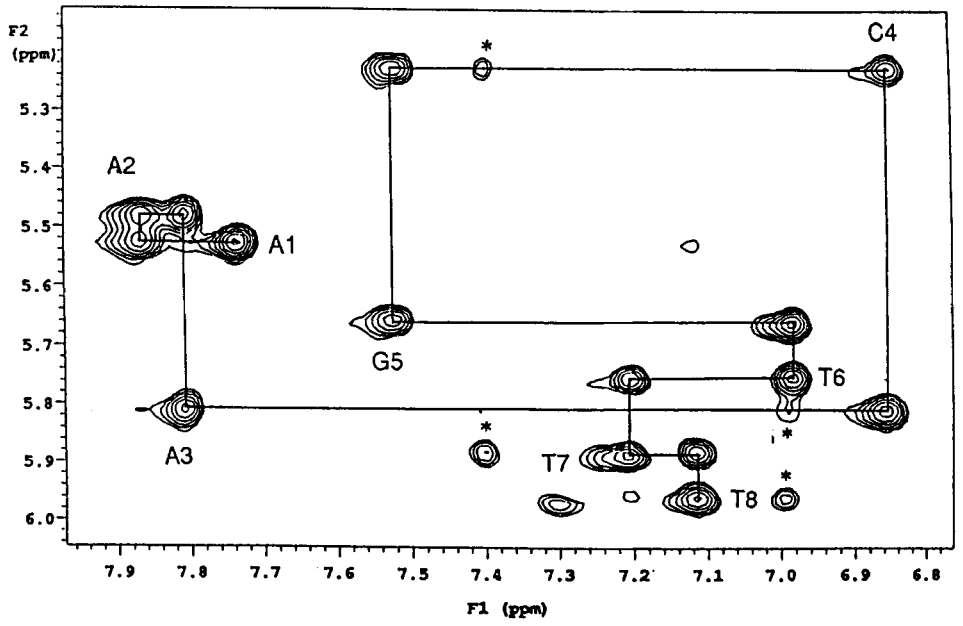


**Figure 4.** Expanded contour plot (H1'-aromatic region) of the phase-sensitive NOESY spectrum (mixing time 150 ms) of (AAACGTTT) in $D_2O$ buffer, pH 6, 10°C. NOEs characteristic of purine tracts are marked with an asterisk.



represent expanded regions taken from the aromatic-H1' portion of the phase-sensitive NOESY experiment. The cross-peaks generated by the dG octamer (Figure 4) are all very similar in intensity. This indicates the duplex takes on a regular structure as is expected in normal B-DNA. However, examination of the same region of the NOESY generated with the ds$^6$G octamer (Figure 5) reveals a structure that is quite irregular. The cross-peaks presented in the aromatic-H1' region of the ds$^6$G octamer cover a wide range of volumes. This indicates the distances between the H1' sugar protons and the base protons are not equivalent. It is especially interesting to note the size of the cross-peaks generated by $C_4$. The distances between the H1' of $C_4$ and its own H6, as well as the distance between the H1' of $C_4$ and the H8 derived from ds$^6$G, appear to be much longer than in the dG octamer thereby generating a smaller NOESY cross-peak. The relative size of the NOE intensities were confirmed by carrying out a NOESY experiment with a mixing time of 50 ms, thus eliminating any NOE intensity distortions arising from spin diffusion. This increase in distance seems to indicate there are significant structural changes in dC-ds$^6$G versus the dG-dC base pairs.

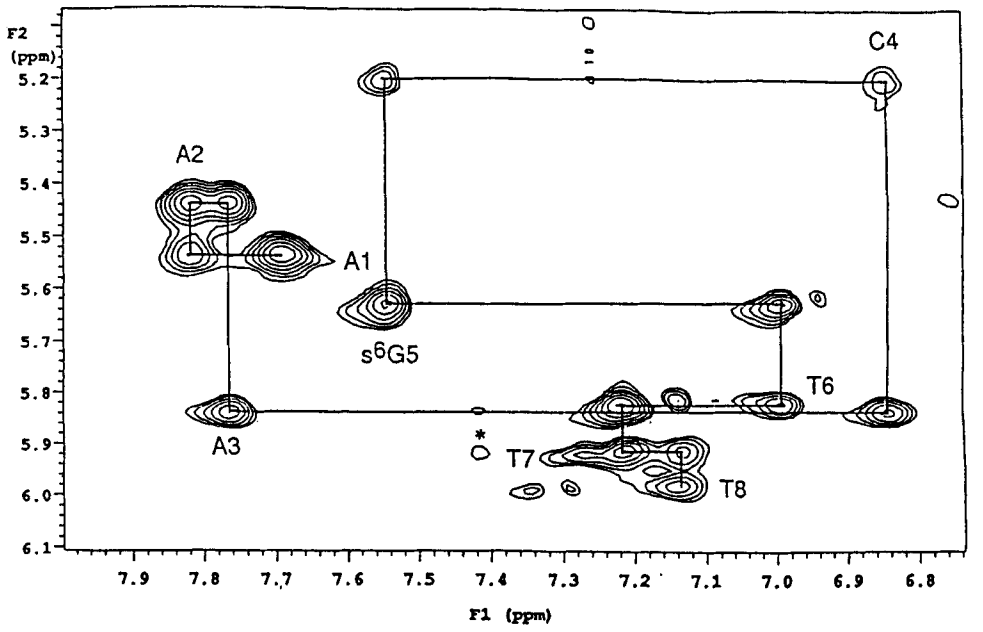


**Figure 5.** Expanded contour plot (H1'-aromatic region) of the phase-sensitive NOESY spectrum (mixing time 150 ms) of (AAACs$^6$GTTT) in $D_2O$ buffer, pH 6, 10°C. NOEs characteristics of purine tracts are marked with an asterisk.



Another unusual feature in the H1'-aromatic region of the ds$^6$G octamer NOESY is that the internucleotide connectivity for the H6 of $C_4$ proton to the H1' proton of its 5' neighbor $A_3$ is significantly stronger than the intranucleotide connectivity for the H6 of $C_4$ proton to its own H1' proton. In normal B-DNA, the internucleotide NOE derived from the aromatic of a given base to the H1' proton of its 5' neighbor is less intense than the intranucleotide NOE from the base to its own H1' proton. Examination of the NOE intensities derived from the dG octamer presented in Figure 4 indicates the aromatic to H1' connectivities for $C_4$ produce similar NOE intensities, indicating the change in NOE intensities observed for the ds$^6$G octamer arises from the incorporation of ds$^6$G and is not derived from a structural irregularity inherent in the sequence.

This reversal of the expected NOE intensities observed in the ds$^6$G octamer indicates the possibility of a change in sugar conformation for the $C_4$ nucleotide. Previous work has indicated a C3'-endo sugar geometry is consistent with the observed reversal of intra/internucleotide NOE intensities.[17] To investigate further the potential change in sugar conforma-

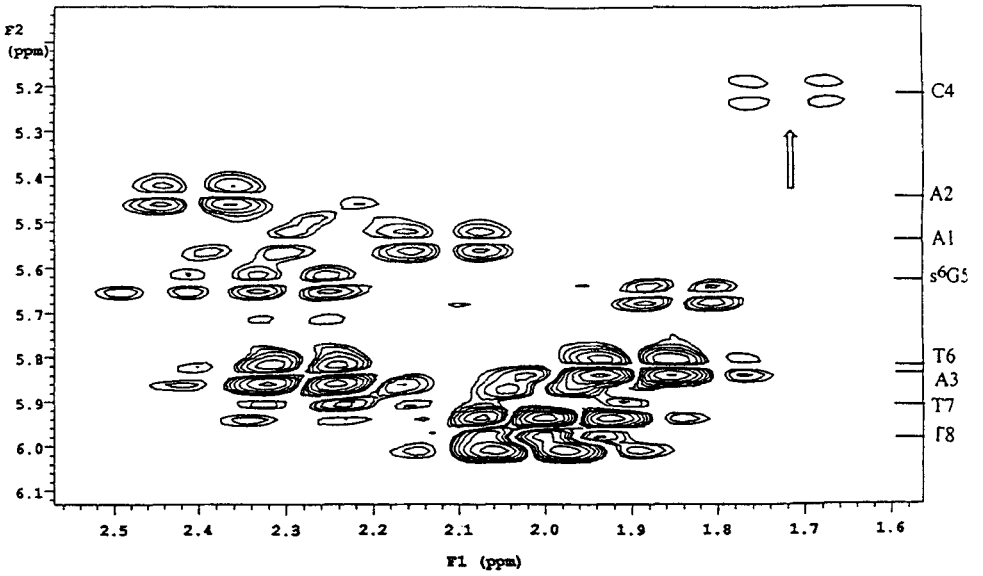


Figure 6. Expanded contour plot (H1'-H2',2" region) of the phase sensitive DQF-COSY spectrum of (AAACs$^6$GTTT) in $D_2O$ buffer, pH6, 10°C. H1'-H2' coupling for C4 is indicated with an arrow.



tion at the $C_4$ position, both the dG and ds$^6$G octamers were subjected to the DQF-COSY 2D-NMR experiment.

The DQF-COSY experiment allows one to evaluate the J-coupling of the sugar protons present in the deoxyribose ring of the octamers which are strongly dependent on the sugar conformation. If the presence of the ds$^6$G residue in the ds$^6$G octamer induces a change in sugar conformation, as the NOESY results indicate, this should be reflected by a change in the coupling constants of the deoxyribose protons of $C_4$.

Previous work has shown that the intensities of the cross-peaks in a DQF-COSY spectrum are proportional to the values of the couplings constants (J) between the two involved nuclei.[18] The results of the DQF-COSY experiment for the ds$^6$G octamer are shown in Figure 6. Comparison of the H1'-H2' and H1'-H2" scalar coupling presented in Figure 6 indicates that the sugar protons of $C_4$ exhibit very weak couplings (indicated by arrow in Figure 6) when compared with the other couplings present in the contour plot. This result, indicating a small H1'-H2' coupling constant, is consistent with the C3'-endo sugar conformation at C4.[19,20]

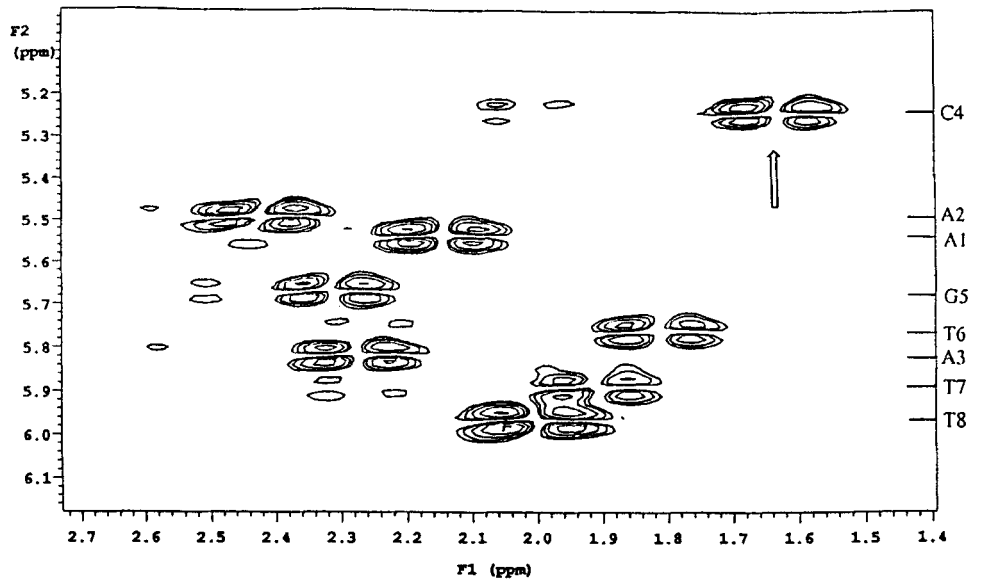


Figure 7. Expanded contour plot (H1'-H2',2" region) of the phase sensitive DQF-COSY spectrum of (AAACGTTT) in $D_2O$ buffer, pH6, 10°C. H1'-H2' coupling for C4 is indicated with an arrow.



In an attempt to confirm that this apparent change in sugar geometry is a result of ds$^6$G incorporation, the dG octamer was subjected to the DQF-COSY experiment. The results of this experiment are shown in Figure 7. The contour plot of the H1'-H2',2" region indicates the H1'-H2' $C_4$ sugar protons (indicated by the arrow in Figure 7) of the dG octamer are strongly coupled, as would be expected in normal B-DNA with the sugar assuming a C2'-endo conformation.[15,17] Thus, the spectral irregularities are present in both the NOESY and DQF-COSY spectra of the ds$^6$G octamer are a result of a change in sugar conformation at $C_4$ induced by the presence of the ds$^6$G-dC base pair in the center of the ds$^6$G octamer.

In an attempt to assess the effects on ds$^6$G incorporation on the structure of the phosphate backbone, both of the octamers were examined by one-dimensional $^{31}$P NMR. Previous work has shown that the $^{31}$P resonances of DNA duplexes are sensitive to local sequence-specific distortions in duplex geometry.[21] Deviations from normal duplex geometry are indicated by upfield shifts of individual $^{31}$P resonance lines. Examination of $^{31}$P spectra derived from the dG and ds$^6$G octamers in 100% $D_2O$ buffered (pH 6) solutions at 10°C indicate the phosphorus backbones of the two octamers are quite similar in structure. Al-

though there are chemical shift differences between the dG and ds$^6$G octamers, including a slight upfield shift of a $^{31}$P resonance line in the ds$^6$G octamer, these chemical shift differences were not large enough to indicate a significant change in the backbone structure of the two octamers.

Further examination of the expanded H1'-aromatic contour plots derived from the dG and ds$^6$G octamers indicates the presence of more extensive structural differences in the two octamers. Close inspection of the contour plot derived from the dG octamer in Figure 4 indicates the presence of several connectivities not expected in normal B-DNA. Each of four unexpected connectivities has been marked in Figure 4 with an asterisk. It is interesting to note these unexpected connectivities are coincident with the chemical shift of H1' protons of $A_3$, $C_4$, $T_7$, and $T_8$. In an attempt to explain the origin of these connectivities, the effects of the chosen sequence d(AAACGTTT) on the structure and expected NOESY connectivities of the octamer were investigated.



It was soon learned that the presence of three contiguous dA residues in the sequence of the octamer could have significant effects on its structure. A large body of work has established that the presence of contiguous dA residues is closely associated with deviations from "pure" B-DNA geometry.[22,23]

Examination of several DNA sequences containing contiguous dA residues with 2-D NMR spectroscopy, specifically the NOESY experiment, has identified several specific NOE connectivities closely associated with purine tracts in DNA.[24,25] This work has shown that the pronounced propeller twist present in such tracts appears to be manifested by observations of NOE between dA-H2 and deoxyribose H1' protons. More specifically, NOE characteristic of purine tracts have been shown to arise from the dA-H2 proton to the H1' proton of the 3' neighbor on the same strand and to the H1' proton of the 3' neighbor on the complementary strand. Each dA-H2 proton thereby generates two NOE, one to the same strand and one across the strand. Given the sequence of the dG octamer, d($A_1A_2A_3C_4G_5T_6T_7T_8$), signals associated with a dA tract would be manifested by NOE from the $A_3$-H2 proton to the H1' of $C_4$ and to the H1' proton of $T_7$, as well as NOE from the $A_2$-H2 to the H1' proton of $T_6$ and to the H1' proton of $T_8$.

Examination of the expanded NOESY contour plot derived from the dG octamer in Figure 4 indicates each of the NOE characteristic of the dA tract is present in the spectrum. It is interesting to note that each of the previously unexpected NOE, marked with an asterisk in Figure 4, arises at the $A_2$ and $A_3$ residues. This information allows the assignment of

the $A_2$-H2 proton at 7.4 ppm, and the $A_3$-H2 proton at 7.0 ppm, as well as providing an interesting structural parameter for the comparison of the dG and the $ds^6G$ octamers.

The $ds^6G$ octamer was assessed for purine tract geometry by evaluating the presence or absence of the characteristic NOE present in the expanded NOESY contour plot of the $ds^6G$ octamer as shown in Figure 5. It is clear from Figure 5 the $ds^6G$ octamer does not assume a structure consistent with a typical dA tract. Only one of the NOE characteristics at $A_3$ is present in the NOESY, while both of the NOE at $A_2$ are completely absent from the spectrum. It is also interesting to note the NOE arising from the $A_3$-H2 proton to the H1' proton of $T_7$ is very small in size when compared to the same NOE present in the dG octamer spectrum shown in Figure 5. Based on this evidence, it appears the presence of $ds^6G$ in the octamer not only leads to a change in the sugar geometry of its base-paired partner, but it also changes the overall shape of the entire octamer when compared to the structure of the dG octamer. This finding has interesting implications when one considers how the replacement of dG with $ds^6G$ would effect the ability of a protein to recognize a given DNA sequence.



**UV Spectroscopy**

To characterize further the effect of $ds^6G$ incorporation on duplex stability, we attempted to use temperature-dependent UV spectroscopy. The octamers were dissolved in 20 mM sodium phosphate buffer (pH 7) and various sodium chloride concentrations, annealed by heating to 50°C and cooling to room temperature and placed in a $T_m$ cell.

The $T_m$ analysis was performed by cooling the sample to 6°C, then heating the cell at a constant rate (0.5°C/min) while monitoring the absorbance at 260 nm. The melting is characterized by an increase in absorbance caused by the cooperative unstacking of the bases present in the oligomer. Attempts to determine the $T_m$ for the $ds^6G$ octamer by monitoring the absorbance at 260 nm gave inconsistent results, a problem which had been previously noted, without explanation, by Rapaport.[26] Since we were interested in the effect of the $ds^6G$ on duplex stability, we chose to monitor absorbance at 340 nm, the $\lambda_{max}$ for $ds^6G$. It was clear from the plot of absorbance versus temperature shown in Figure 8, that as the cell was heated above 20°C the thione chromophore of $ds^6G$ was being lost. The lability of 6-thioguanosine under alkaline conditions had been well characterized but the instability at pH 7 was not anticipated.[10] It should be noted in this context that the NMR data described above were collected at 10°C; no detectable thione loss was observed at that

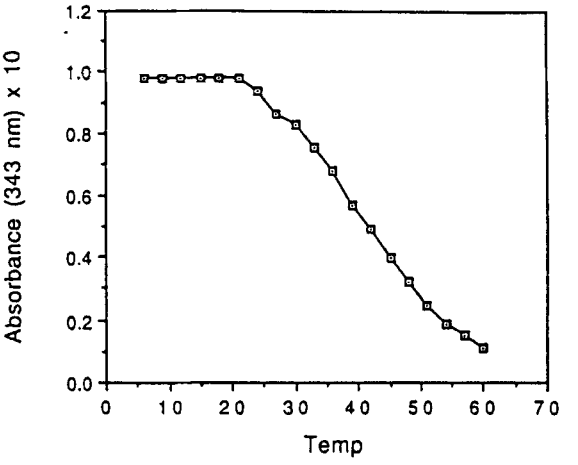


Figure 8. Temperature dependence of the 343 nm absorbance of (AAACs$^6$GTTT) in 0.1 M NaCl 20 mM buffer (pH7).



temperature. We had previously found that $H_2S$ protected 6-thioguanosine from oxidative loss under alkaline conditions, but its volatility precluded its use at elevated temperatures.

Conditions where the thione chromophore of ds$^6$G was stable were investigated. The $T_m$ of the ds$^6$G octamer is monitored at 340 nm in three different solutions: pH 7 buffered sodium phosphate, pH 6 buffered sodium phosphate, and pH 7 buffered sodium phosphate containing 10 mM dithiothreitol (DTT). The addition of DTT was anticipated to prevent oxidative loss of the thione chromophore of ds$^6$G by acting as an antioxidant. It is clear from the results of this study the pH 6 and pH 7 buffered solutions suffer significant loss of the thione chromophore while the solution containing 10 mM DTT was protected. HPLC analysis of the three solutions confirmed the fact that in the buffered solution there was significant conversion of the s$^6$G octamer into the dG octamer. In the pH 7 buffer, the conversion approached 80% while in the case of the pH 6 buffer there was approximately 30% conversion. HPLC analysis of the solution containing 10 mM DTT did not detect any conversion to the dG octamer. Later work indicated that a 1 mM concentration of DTT was sufficient to prevent oxidative loss of the thione chromophore present in ds$^6$G. This result has been confirmed by HPLC. Thermal melting studies utilizing the buffers containing 1.0 mM DTT indicate that the ds$^6$G octamer melted with an average $T_m$ that is 10°C lower than that of the dG octamer in pH 6 sodium phosphate buffer with 0.1 M added NaCl, in good agreement with data derived from one-dimensional NMR studies.

It has been shown that the incorporation of $ds^6G$ into an oligonucleotide leads to significant structural changes easily observable by NMR. It is apparent the structural changes involve disruption of adjacent base pairs as well as the $ds^6G$-dC base pair itself. This results in a significant decrease in duplex stability as measured by the line width of imino protons involved in hydrogen bonds. It has also been shown through the addition of DTT, the lability of the thione present in the $ds^6G$ chromophore can be overcome. This should allow biochemical studies to be performed on $ds^6G$ containing oligonucleotides without the possibility of degradation. Based on these results, incorporation of a single $ds^6G$ residue can have a fairly dramatic effect on the local structure of a given DNA sequence. It is tempting to hypothesize that these structural perturbations induced by the presence of $ds^6G$ are related to the anticancer effects of 6-thioguanine. Disruptions in DNA-protein interactions necessary for cell survival and proliferation would clearly be a plausible implication of $ds^6G$ incorporation based on this work's results.



## ACKNOWLEDGMENTS

We wish to thank Dr. Darrell R. Davis and Jay olsen for their helpful discussion and assistance in acquiring and analyzing the NMR data.

This work was supported in part by a grant from NIH (RO1 AI27692). The DNA syntheses and NMR studies owe partial support to the Utah Regional Cancer Center Core grant P30 CA42014. Provision of a graduate fellowship to Michael Christopherson by the University of Utah Research Committee is gratefully acknowledged.

## REFERENCES

1. Kovach, J.S.; Rubin, J.; Creagan, E.T.; Schutt, A.J.; Kvols, L.K.; Swingen, P.A; Hu, T.C. *Cancer Res.* **1986**, *46*, 5959.
2. LePage, G.A.; Jones, M. *Cancer Res.* **1961**, *21*, 1590.
3. Nelson, J.A.; Carpenter, J.W.; Rose, L.M.; Adamson, D.J. *Cancer Res.* **1975**, *35*, 2872.
4. Lee, S.H.; Sartorelli, A.C. *Cancer Biochem. Biophys.* **1981**, *5*, 189.
5. Christie, N.T.; Drake, S.; Meyn, R.E.; Nelson, J.A. *Cancer Res.* **1981**, *44*, 3665.
6. Hori, H. *Mie Med. J.* **1990**, *40*, 99.
7. Nelson, J.A.; Pan, B.F.; Priebe, T.S. *Proc. Amer. Soc. Cancer Res.* **1991**, *32*, 2119.
8. Amarnath, V.; Broom, A.D. *Biochemistry* **1976**, *15*, 4286.

9. Bugg, C.E.; Thewalt, U. *J. Amer. Chem. Soc.* **1970, *92*** 7441.

10. Christopherson, M.S.; Broom, A.D. *Nucl. Acids. Res.* **1991**, *19*, 5719.

11. Waters, T.R.; Connolly, B.A. *Nucleosides and Nucleotides* **1992,** *11*, 1561.

12. Xu, Y.-Z.; Zheng, Q.; Swann, P.F. *Tetrahedron* **1992**, *48*, 1729.

13. Hare, D.R.; Wemmer, D.E.; Chou, S.; Drobny, G.; Reid, B.R. *J. Mol. Biol.* **1983**, *171*, 319.

14. Bower, M.; Summers, M.F.; Kell, B.; Hoskins, J.; Zon, G.; Wilson, W.D. *Nucl. Acids Res.* **1987**, *15*, 3531.

15. Schaefer, T.; Parr, W.J.E. *Can. J. Chem.* **1977**, *55*, 3732.

16. Dudek, E.P.; Dudek, G. *J. Org. Chem.* **1967**, *32*, 823.

17. Lin, C.H.; Hill, G.C.; Hurley, L.H. *Chem. Res. Toxicol.* **1992**, *5*, 167.

18. Hosur, R.V.; Ravinkumar, M.; Chary, K.V.R.; Sheth, A.; Govlin, G.; Zu-Kun, T.; Miles, H.T. *FEBS Lett.* **1986**, *205*, 71.

19. Wüthrich, K. *NMR of Proteins and Nucleic Acids*; John Wiley and Sons: New York, 1986.

20. Chary, K.V.R.; Hosur, R.V.; Govil, G.; Zu-Kun, T.; Miles, H.T. *Biochemistry* **1987**, *26*, 1315.

21. Eckstein, F.; Jovin, T.M. *Biochemistry* **1983**, *22*, 4546.

22. Marini, J.C.; Levene, S.D.; Crothers, D.M.; Englund, P.T. *Proc. Natl. Acad. Sci.* **1982**, *79*, 7664.

23. Wu, H.; Crothers, D.M. *Nature* **1984**, *308* 509.

24. Kintar, A.; Klevit, R.E.; Reid, B.R. *Nucl. Acids Res.* **1987**, *15*, 5845.

25. Celda, B.; Widmer, H.; Leupin, W.; Chazin, W.J.; Denny, W.A.; Wüthrich, K. *Biochemistry* **1989**, *28*, 1462.

26. Rapaport, H.P. *Nucl. Acids. Res.* **1988**, *16*, 7253.

Received 9/1/93
Accepted 9/30/93